OPEN BIOLOGY

royalsocietypublishing.org/journal/rsob

Research

Cite this article: Fitz-James M, Sparrow P, Paton C, Sarkies P. 2025 Polycomb-mediated transgenerational epigenetic inheritance of *Drosophila* eye colour is independent of small RNAs. *Open Biol.* **15**: 240298.
https://doi.org/10.1098/rsob.240298

Received: 11 October 2024
Accepted: 1 February 2025

Subject Areas:
biochemistry, molecular biology, genetics

Keywords:
open biology, biorxiv, research, epigenetics, siRNA, transgenerational epigenetic inheritance

Author for correspondence:
Peter Sarkies
e-mail: peter.sarkies@bioch.ox.ac.uk

Electronic supplementary material is available online at https://doi.org/10.6084/m9.figshare.c.7702725.

THE ROYAL SOCIETY PUBLISHING

Polycomb-mediated transgenerational epigenetic inheritance of *Drosophila* eye colour is independent of small RNAs

Maximilian Fitz-James, Poppy Sparrow, Christopher Paton and Peter Sarkies

University of Oxford, Oxford, UK

PS, 0000-0003-0279-6199

Transgenerational epigenetic inheritance (TEI) describes the process whereby distinct epigenetic states are transmitted between generations, resulting in heritable gene expression and phenotypic differences that are independent of DNA sequence variation. Chromatin modifications have been demonstrated to be important in TEI; however, the extent to which they require other signals to establish and maintain epigenetic states is still unclear. Here we investigate whether small non-coding RNAs contribute to different epigenetic states of the Fab2L transgene in *Drosophila* triggered by transient long-range chromosomal contacts, which requires Polycomb complex activity to deposit the H3K27me3 modification for long-term TEI. By analysing mutants deficient in small non-coding RNAs, high-throughput sequencing data, long-range chromosomal contacts and gene expression, we demonstrate that small non-coding RNAs do not contribute directly to initiation or maintenance of silencing. However, we uncover an indirect role for microRNA expression in transgene silencing through effects on the Polycomb group gene *Pleiohomeotic*. Additionally, we show that a commonly used marker gene, *Stubble* (*Sb*), affects *Pleiohomeotic* expression, which may be important in interpreting experiments assaying Polycomb function in *Drosophila* development. By ruling out a plausible candidate for TEI at the Fab2L transgene, our work highlights the variability in different modes of TEI across species.

1. Introduction

In addition to the core genetic information encoded in DNA, eukaryotes possess several layers of epigenetic information which affect gene expression without altering DNA sequence [1]. This epigenetic information includes signals such as DNA methylation [2], histone modifications [3] and small non-coding RNAs (sRNAs) [4], which form a key part of gene regulatory pathways in both development and adaptation, contributing to differences between cells within an individual as well as between individuals within a population. Often, multiple epigenetic mechanisms combine to produce robust epigenetic states [5].

In some cases, epigenetic information can be transmitted through the germline to subsequent generations in a process known as transgenerational epigenetic inheritance (TEI) [6]. While the precise mechanism by which these epigenetic signals are inherited is often unclear, proposed mechanisms usually invoke either the direct 'replicative' inheritance of the signal through the gametes, or a form of indirect, 'reconstructive' inheritance whereby one signal is erased during development but reconstructed later from a different, directly inherited signal [7].

sRNAs have been implicated in many of the best-described mechanisms of TEI [8–13]. In some organisms, they also have well-described mechanisms of gametic transmission [12,14,15] and self-propagation [16,17]. As a result,

sRNAs are often considered the primary inherited signal in many examples of TEI. In *Drosophila melanogaster*, the major classes of sRNAs are 22-nucleotide (22 nt) micro-RNAs (miRNAs), which recognize transcripts through short complementary base pairing target sites in the mRNA 3′-untranslated region [18], 21–24 nt small interfering RNAs (siRNAs), which silence target transcripts via the RNA-induced silencing complex [17,19], and 22–28 nt piwi-interacting RNAs (piRNAs), responsible for both transcriptional and post-transcriptional silencing of transposable elements [19–21].

The mechanisms whereby sRNAs contribute to TEI are best described in *Caenorhabditis elegans*. Key to this is the activity of RNA-dependent RNA polymerases that synthesize a type of sRNA known as 22G-RNAs. 22G-RNAs in association with Argonaute proteins, notably the nuclear Argonaute HRDE-1, can be transmitted through the germline and recruit RNA-dependent RNA polymerase, leading to the synthesis of more 22G-RNAs and thus stable epigenetic memory. Initial targeting of 22G-RNAs is often kick-started by piRNA targeting, providing a mechanism whereby piRNAs can initiate stable silencing that can last even if piRNAs are removed [22–24].

Drosophila melanogaster does not have RNA-dependent RNA polymerase. Nevertheless, piRNA-mediated silencing of transposons in *Drosophila*, which operates partly through recruitment of the repressive histone modification H3K9me3, has also been shown to be transgenerationally inherited [25,26]. Some other cases of TEI in *Drosophila*, however, have reported the inheritance of histone modifications not usually associated with sRNA-directed silencing, in particular H3K27me3 [27–29]. The potential involvement of sRNAs in these cases has yet to be fully explored and is an important step in determining if these histone modifications can truly be inherited directly, rather than simply acting as secondary signals reconstructed from inherited sRNAs.

One such case is the transgenic *Drosophila* line Fab2L [30,31]. This line displays TEI involving either the silencing or activation of a transgenic region including a *mini-white* reporter gene, responsible for pigmentation in the adult eye. While eye colour is initially highly variable, these flies can be selected to produce genetically identical 'epilines' with either fully white or fully red eyes [29]. Once established, these epilines can be maintained for many generations (>100) in the absence of selection. The primary epigenetic signal responsible for these phenotypic differences has been identified as the histone modification H3K27me3, deposited by the Polycomb repressive complex 2 (PRC2). Many analogous systems where chromatin modifications are inherited transgenerationally require sRNAs in addition to ensure robust transmission of the epigenetic state, notably at the fission yeast centromere [32]. However, the potential involvement of sRNAs in PRC2-dependent TEI in *Drosophila* has not been explored.

In order to investigate the potential involvement of sRNAs in this case of TEI, we performed small RNA sequencing (sRNA-seq) in several different Fab2L lines as well as analyses of Fab2L lines bearing mutations in key sRNA pathway genes. We detected no evidence of sRNAs mapping to the Fab2L transgene, nor any effect of most sRNA mutations on eye colour, its inheritance or the expression of key genes involved in Fab2L TEI. We thus conclude that sRNAs do not play a role in the epigenetic phenotypes of the Fab2L line. However, we report a novel effect of the *Sb[1]* mutation on the expression of the PRC2 recruiter *Pleiohomeotic* (*Pho*), which may have wider-ranging implications for the interpretation of results involving this widely used genetic marker in other studies involving Polycomb targets.

2. Results and discussion

2.1. Small RNAs do not contribute to phenotypic differences between genetically identical epilines

The *Drosophila* Fab2L line carries a single copy of 12.4 kb transgene inserted into chromosome 2 [29,30]. This transgene contains the reporter genes *LacZ* and *mini-white* under the control of the *Fab-7* regulatory element, which is also present endogenously on chromosome 3. The *mini-white* reporter gene, which controls red pigment deposition in the eye, is not expressed uniformly in Fab2L flies but shows a mosaic pattern of eye pigmentation, with some ommatidia showing strong *mini-white* expression and others strong repression (figure 1*a*). This variability is attributed to the stochastic binding of the PRC2 to the *Fab-7* element, which deposits the repressive histone modification H3K27me3 to randomly silence the transgene during development in some cells, but not in others [29,33].

Transgenerational inheritance of these epigenetic differences over the transgene can lead to the establishment through artificial selection of genetically identical but phenotypically distinct 'epilines': populations of flies in which all individuals have either fully red or fully white eyes (figure 1*a*). Phenotypic differences between these epilines correlate with different levels of H3K27me3 across the transgene, both in the adult head and in the embryo [29]. However, to date, no other epigenetic differences between the epilines have been identified, nor has a potential role for small RNAs been tested.

To determine if small RNAs contribute to the phenotypic differences between Fab2L-W* (white-eyed) and Fab2L-R* (red-eyed) epilines, we performed sRNA-seq in embryos from both of these epilines, as well as from unselected mosaic Fab2L flies. Despite good coverage of the genome as a whole and many 21–28 nt reads corresponding to the expected length of sRNAs mapping to expected targets such as hairpin RNA loci and piRNA clusters (electronic supplementary material, materials S1 and S2), almost no sRNA transcripts mapped to either the transgene or the endogenous *Fab-7* element in any of the lines (figure 1*b*). This indicates that there is no direct targeting of the Fab2L locus or its transcripts by sRNAs. Given that all previous examples of sRNA-mediated epigenetic inheritance involved direct targeting of the locus by sRNAs [34,35], the absence of sRNAs indicated that they were unlikely to contribute to the heritable epigenetic differences in eye colour between these populations.

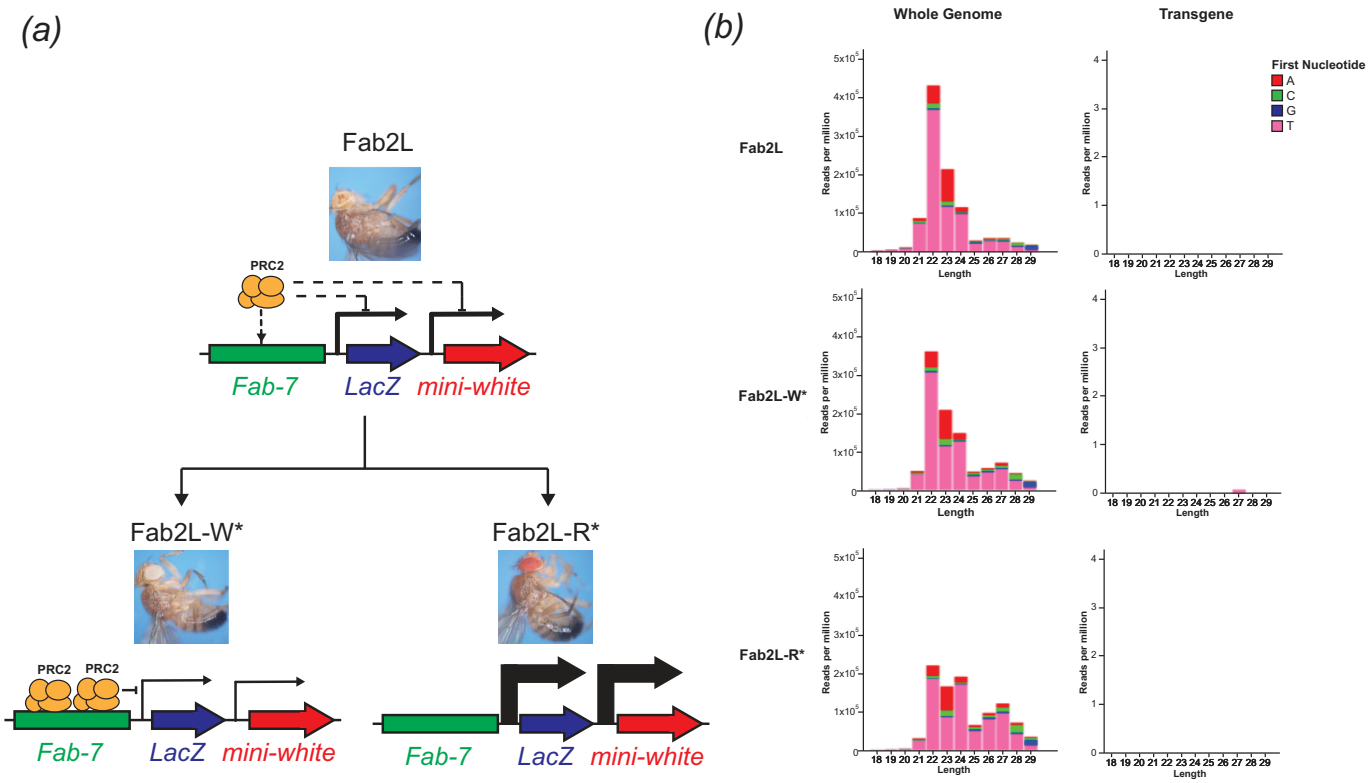

Figure 1. No small RNAs map to the Fab2L transgene in either naïve flies or epilines. (*a*) Schematic of the Fab2L transgene, containing *LacZ* and *mini-white* reporter genes under control of the *Fab-7* regulatory element. Stochastic binding of PRC2 to *Fab-7* leads to random inactivation of the transgene, resulting in a mosaic eye colour which can be selected to produce either fully white or fully red-eyed fly lines. (*b*) sRNA-seq in embryos of the indicated genotypes. 18–29 nt reads were mapped to either the whole *Drosophila* genome (left) or the Fab2L transgene sequence (right). This latter includes the *Fab-7* element with homology to the endogenous *Fab-7*, thus any reads mapping to the endogenous sequence would also map to the transgene. Colours indicate the first nucleotide of each read.

2.2. Initiation of epigenetic inheritance through chromatin contacts does not involve small RNAs

We next sought to determine whether small RNAs might contribute to the initiation of epigenetic inheritance. Epigenetic inheritance of eye colour in Fab2L does not happen spontaneously but requires a triggering event. Indeed, in a 'naïve' Fab2L population, eye colour is not heritable (figure 2*a*). Epigenetic inheritance can be established by introducing a single generation of heterozygosity at the endogenous *Fab-7* locus [29]. After this transient genetic change, the resultant Fab2L flies, although genetically identical to the naïve Fab2L line, now have heritable eye colour and can be selected to produce epilines with either red or white eyes (figure 2*b*). Previous work has shown that the establishment of TEI involves chromatin contacts between the transgenic and endogenous *Fab-7* elements, which are present in Fab2L flies and increase even further upon *Fab-7* heterozygosity. These contacts alone are sufficient to trigger TEI but are not required for the maintenance of heritable eye colour differences [33]. Furthermore, sRNA pathways were previously implicated in contacts between *Fab-7* elements in a related fly line carrying an X-chromosome transgene [36]. In this study, mutation of various sRNA pathway genes was found to decrease contacts between the *Fab-7* elements [36]. We therefore asked if similar processes in the Fab2L line could result in small RNAs contributing to the initiation, rather than the maintenance, of heritable epigenetic changes.

To test this, we performed sRNA-seq on Fab2L; *Fab7[1]*/+ embryos heterozygous for the endogenous *Fab-7* and corresponding to the time period when epigenetic inheritance is initiated (figure 2*c*; electronic supplementary material, figure S3). We did not detect small RNA transcripts mapping to either the transgene or the endogenous *Fab-7*, arguing against the involvement of small RNAs in the initiation of TEI.

To test these conclusions further, we examined the effects of mutations that disrupt small RNA pathways on the Fab2L-*Fab7* chromatin contacts that are essential for TEI initiation. We performed fluorescence *in situ* hybridization (FISH) on embryos using probes that highlight the regions surrounding the *Fab-7* elements (figure 2*d*). As previously reported, these two regions frequently colocalize in the nuclei of Fab2L embryos, but not in Fab2L; *Fab7[1]* embryos that lack the endogenous *Fab-7*, resulting in a significant decrease in the average distance between the two loci measured across many nuclei (figure 2*e*; $p < 5 \times 10^{-6}$, Tukey's HSD after two-way ANOVA). We then looked at the frequency of contacts in Fab2L embryos carrying homozygous loss-of-function mutations in three genes with major roles in each of the three small RNA pathways. These were *Argonaute 2* (*AGO2*, required for siRNA-directed silencing [37]), *armitage* (*armi*, required for piRNA biogenesis [38–40]) and *Dicer-1* (*Dcr-1*, required for miRNA biogenesis [41]). All three mutant embryos showed a similar frequency of contacts to the wild-type Fab2L embryos (figure 2*d,e*). Accordingly, we also found no effect of any of these mutations on the expression of the gene *Trithorax-like* (*Trl*), also known as *GAGA-Factor* (*GAF*), which was previously shown to be the primary factor driving the contacts between the transgenic and endogenous *Fab-7* elements (figure 2*f*).

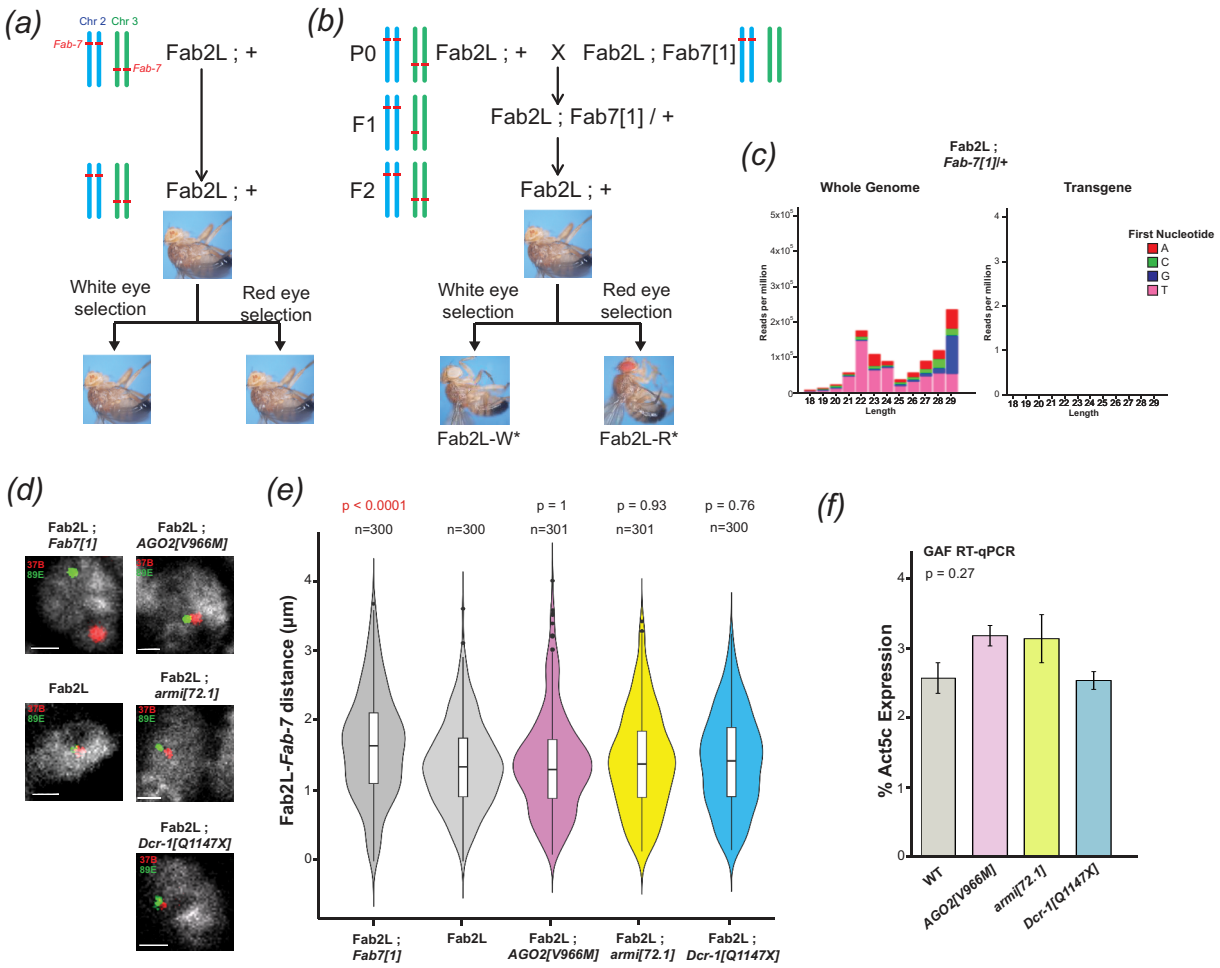

Figure 2. Small RNA pathways do not contribute to TEI establishment either in concert with or independently from chromatin contacts. (*a,b*) Crossing scheme for the triggering of TEI at Fab2L, with diagrammatic representation of the copy number of the *Fab-7* element on chromosomes 2 and 3. Heterozygosity of the endogenous Fab-7 on chromosome 3 leads to the establishment of TEI at the transgenic site on chromosome 2, thus enabling the selection of epilines. (*c*) sRNA-seq in Fab2L; *Fab7[1]/+* embryos heterozygous for the endogenous *Fab-7*. 18–29 nt reads were mapped to either the whole *Drosophila* genome (left) or the Fab2L transgene sequence (right). Colours indicate the first nucleotide of each read. (*d*) Illustrative micrographs of FISH in embryonic nuclei of the indicated genotypes. Nuclei are stained with DAPI, the 37B locus surrounding the Fab2L transgene is stained in red and the 89E locus surrounding the endogenous *Fab-7* is stained in green. Scale bars represent 1 µm. (*e*) Violin plots representing the distribution of average distance between the 37B and 89E regions surrounding the Fab2L transgene and endogenous *Fab-7*, respectively, as determined by FISH in the indicated genotypes. Distances were measured in stage 14–15 embryos in T1 and T2 segments. Significance was determined by two-way ANOVA, with distributions compared using Tukey's HSD (n.s. = $p > 0.1$). (*f*) RT-qPCR for expression of GAF in Fab2L embryos homozygous for the indicated mutations. Expression was normalized to Act5C and overall significance was tested by one-way ANOVA.

Taken together, these results indicate that small RNAs are not involved in the initiation of TEI, either through direct effects on the transgene or indirectly by contributing to the previously observed increase in Fab2L–*Fab7* chromatin contacts. Both establishment and inheritance of the Polycomb-dependent epigenetic phenotypes in Fab2L, therefore, appear to be independent of sRNA pathways.

2.3. Horizontal transfer of epigenetic state by paramutation is independent of small RNAs

The epigenetic state of the Fab2L transgene can be transmitted horizontally between alleles by the process of 'paramutation' [29]. Paramutation denotes a type of non-Mendelian inheritance whereby an epigenetic state is transmitted *in trans* between two homologous alleles [42]. In the Fab2L line, crossing a naïve Fab2L with an established Fab2L epiline (either white or red-eyed) can result in the naïve allele acquiring the altered epigenetic state of the epiline allele. This phenomenon can be tracked by the use of a recessive *black[1]* marker allele, closely linked to the Fab2L transgene, such that F2 individuals that have inherited both copies of Fab2L from the naïve parent can be determined with high probability (electronic supplementary material, figure S4). Although these F2 flies possess the genetic material of the naïve P0 population, the majority have an epigenetic state more closely resembling that of the epiline with which it was crossed, demonstrating that they have acquired a new epigenetic state.

Although the term 'paramutation' denotes a pattern of inheritance, rather than a specific molecular mechanism, small RNAs have been implicated in paramutation in many organisms, including *Drosophila* [34,43]. As free-floating molecules, sRNAs produced by one allele are able to target and silence both alleles, thus acting as carriers of epigenetic information that transmit epigenetic state from one allele to the other. sRNAs produced from the newly silenced allele can in turn silence other alleles in future generations, resulting in propagation of the epigenetic state between alleles *in trans*. Thus, while the mechanisms of

paramutation vary to an extent, the involvement of sRNAs is universal in all well-described cases [42]. However, the observed lack of sRNAs mapping to the Fab2L transgene led us to question whether sRNAs were responsible for paramutation at this locus.

In order to test the potential role of small RNA pathways in Fab2L paramutation, we performed crosses between Fab2L epilines and naïve Fab2L flies bearing different mutations to determine their effect on the efficiency of paramutation. In each case, we crossed both white and red epilines with a naïve Fab2L line that was both homozygous for the *black[1]* allele (closely linked to the Fab2L transgene) and heterozygous for a mutation balanced on the chromosome 3 balancer TM3-Ser (figure 3*a*). In the F1 generation, we sorted the flies into two populations, those that inherited the balancer and those that inherited the mutation, which were then self-crossed in parallel. The recessive *black[1]* phenotype then allowed us to select for F2 flies from each of these crosses that had inherited both copies of the Fab2L transgene from the naïve parent, which we then scored for eye colour and compared. Thus, the effect of each mutation on the F2 population could be compared to an internal control derived from the same initial P0 cross. This was important, as variations between the eye colours of starting populations can impact the F2 phenotype, making comparisons between crosses unreliable. Differences between these F2 populations would indicate an effect of the mutation on Fab2L eye colour, suggestive of a role for the mutated gene either in the horizontal transfer of epigenetic information by paramutation, or more directly in regulating the expression of the transgene. The magnitude of these differences was expected to vary between females and males, which have described differences in eye colour in the Fab2L line [29,33], and between crosses with white or red-eyed lines, which have more or less complete penetrance of the monochrome eye colour phenotype. We were thus careful to test only comparable F2 populations and judged that a significant difference between any one of these tests would be suggestive of a role for the mutated gene in paramutation or transgene expression.

This experimental set-up imposed constraints on our choice of mutants, as the requirement to independently segregate the mutation and the Fab2L locus prevented us from analysing mutations on chromosome 2 linked to the Fab2L transgene. We therefore performed these crosses with naïve Fab2L flies bearing the previously mentioned loss-of-function mutations for *AGO2*, *armi* and *Dcr-1*, all of which are on chromosome 3. As controls, we performed the same cross with Fab2L flies bearing no mutation on chromosome 3 (wild type) as well as flies mutated for the essential PRC2 component *Enhancer of zeste*, or *E(z)* [44], and the chromatin organizer and insulator *Trl*/*GAF* [45], both of which have important roles in regulating the Fab2L transgene [29,33]. As expected, crossing wild type flies with epilines resulted in F2 flies that had at least partially adopted epiline identity, with a large proportion of the population having fully red or fully white eyes, rather than the near-100% mosaicism observed in a naïve population (figure 3*b*,*c*; electronic supplementary material, figure S5*a*,*b*). More importantly, there was no significant difference between F2 flies that had inherited the balancer and those that had not. Conversely, mutations in both *E(z)* and *Trl* significantly reduced the number of monochrome-eyed flies in at least one of the crosses, compared to flies from the same cross that inherited the balancer ($p < 2 \times 10^{-18}$ and $p < 7 \times 10^{-6}$, respectively, Fisher's exact test), consistent with the known role of these genes in regulating transgene expression.

Several cases of paramutation have implicated siRNAs in plants [42,43] and piRNAs in metazoans, including *Drosophila* [22,24,25,46]. However, neither *AGO2* nor *armi* mutations had any effect on the efficiency of paramutation, arguing against their role in this particular case (figure 3*b*,*c*; electronic supplementary material, figure S5*a*,*b*). Consistent with this, two other mutants in piRNA genes we tested, *maelstrom* (*mael*) [47] and *argonaute 3* (*AGO3*) [48], also had no effect (electronic supplementary material, figure S5*c*,*d*), and we detected no small RNA transcripts mapping to the transgene in the F1 of our paramutation crosses (electronic supplementary material, figure S6). This suggests that paramutation at the Fab2L locus does not occur by the previously described sRNA-dependent mechanism in *Drosophila*, nor does it appear to involve sRNAs at all. Further investigation into the mechanism of this case of paramutation is an interesting direction for future research to explain how epigenetic state can be transmitted *in trans* between alleles without using sRNAs as a carrier of epigenetic information.

Interestingly, however, mutation of *Dcr-1* had a small but measurable effect, most notably in the cross with the red epiline (figure 3*b*). While this difference was no longer statistically significant after adjustment by Bonferroni correction ($p = 0.0075$ before correction, $p = 0.075$ after correction, Fisher's exact test), it remained within the reportable range ($p < 0.1$) and represented a significant enough effect from a heterozygous mutation to merit further investigation.

2.4. The common genetic marker *Stubble* influences Fab2L transgene expression

When initially testing lines containing balancer chromosomes for use as controls, we performed the paramutation cross (figure 3*a*) using both Fab2L, *black[1]*; + / TM3-Ser, bearing the scalloped wing marker due to mutation in the gene *Serrate* [49,50] and Fab2L, *black[1]*; + / TM3-Sb, bearing the shortened bristle phenotype due to the *Sb[1]* mutation in the gene *Stubble* [49,51]. While the former displayed the expected similarities between the F2 populations, leading us to use TM3-Ser in all subsequent crosses (figure 3*b*,*c*), the TM3-Sb containing line did not. Indeed, F2 flies that inherited the TM3-Sb balancer showed a significant shift towards red eyes compared to those that did not ($p = 0.037$ for red cross, $p < 7 \times 10^{-9}$ for white cross, Fisher's exact test; figure 3*d*,*e*; electronic supplementary material, figure S5*e*). To confirm that this difference reflected an effect of the mutation, we performed paramutation crosses with Fab2L flies carrying the *Sb[1]* mutation balanced over TM3-Ser. Once again, F2 flies that inherited the *Sb[1]* mutation showed a significant shift towards red eye colour ($p < 7 \times 10^{-4}$ for red cross, Fisher's exact test; figure 3*d*,*e*; electronic supplementary material, figure S5e). This unexpected result suggested that *Stubble* influenced the regulation of transgene expression in the Fab2L line.

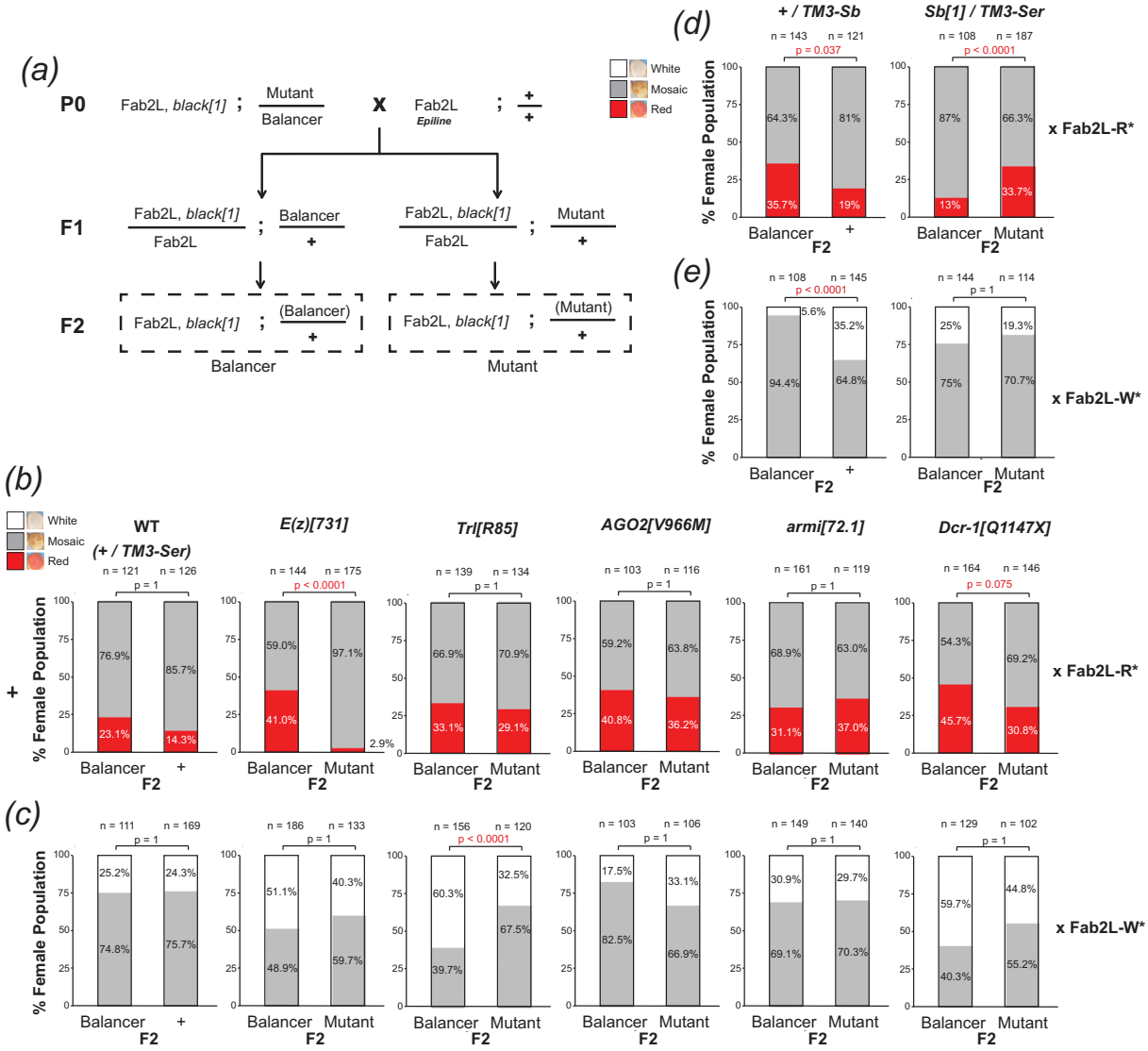

Figure 3. Mutation in *Dcr-1* and *Sb*, but not *AGO2* or *armi*, interfere with paramutation. (*a*) Crossing scheme to test the effect of mutations on the efficiency of paramutation. In each case, naïve Fab2L flies carrying the transgene linked to *black[1]* as well as a chromosome 3 mutation balanced on TM3-Ser were crossed with an established white or red epiline. F2 flies having inherited the transgene from the naïve P0 and the mutation were compared to those that had inherited the naïve transgene and the balancer as an internal control derived from the same cross. (*b–e*) Phenotypic distribution of eye colour in the F2 females of the paramutation crosses. In the P0, naïve Fab2L flies carrying the indicated mutation were crossed with either a red epiline (*b,d*) or a white epiline (*c,e*). In each case, F2 adults from the same cross inheriting either the balancer or mutant were scored for eye colour and compared by Fisher's exact test, with *p* values adjusted by Bonferroni correction (n.s. = $p > 0.1$).

2.5. *Dcr-1* and *Sb* mutations interfere with Polycomb recruitment by downregulating *Pho*

Though we set out to investigate the potential role of sRNAs in TEI at the Fab2L locus, we identified no discernible involvement of the two sRNA pathways most likely to be responsible for heritable epigenetic differences, siRNAs and piRNAs. Instead, we identified potential effects of the miRNA pathway (through mutation of *Dcr-1*) and *Stubble* on the epigenetic eye colour phenotype.

Unlike siRNAs and piRNAs, miRNAs have no known method of self-propagation. They are however major post-transcriptional regulators of a wide array of genes. We reasoned therefore that the observed effect of *Dcr-1* mutation on Fab2L eye colour was unlikely to reflect an involvement in the inheritance of eye colour, but was more likely a secondary effect brought about by misregulation of one of the many miRNA targets. Similarly, *Stubble* is an important signalling protein whose mutation has many downstream effects. Its most clearly defined function is in epithelial morphogenesis, bringing about the visible bristle phenotype frequently used as a marker [51]. However, this function extends more generally to imaginal disc morphogenesis, with known phenotypes in both the leg and wing among others [52–56]. Its role in activating the Rho-GTPase signalling pathway [51] has also linked it to regulation of the Ecdysone receptor [54], a major transcription factor with hundreds of targets across developmental stages [57]. This led us to consider the possibility that mutation of *Sb* might affect transgene expression.

All mutations tested in our previous assays were homozygous lethal, disrupting as they do important genes with essential functions. Our analyses of adult eye colour were therefore limited to determining the effects of heterozygous mutants, which may mask some of the more severe effects of the mutations. All of these mutants, however, survive until at least late embryogenesis, if not the larval stage, allowing us to analyse homozygous mutants at earlier stages of development. To further

investigate the effects of *Dcr-1* and *Sb* mutations, we performed quantitative reverse transcription polymerase chain reaction (RT-qPCR) on Fab2L embryos homozygous for the previously used *Dcr-1* and *Sb* loss-of-function mutations. As controls, we used a naïve Fab2L line, a wild-type w-line, containing no Fab2L transgene or endogenous *white* gene, and a line carrying a previously described mutant version of the Fab2L transgene (labelled here 'Fab2L-constit.') in which the binding sites for the PRC2 recruiters *Pho* and *GAF* are mutated, resulting in constitutive expression of the *mini-white* reporter in the transgene due to absence of PRC2 silencing [33]. We also analysed the *AGO2* and *armi* mutants, which we had determined to have no effect on the transgene based on our paramutation crosses (figure 3*b*,*c*) to determine if homozygosity of these mutants revealed any effects not visible in heterozygotes.

The line carrying the mutated version of Fab2L showed strong expression of both *mini-white* and *LacZ* from the transgene, compared to the much lower but still detectable levels of expression in the unmutated Fab2L (figure 4*a*,*b*). Mutation of *AGO2* or *armi* had no significant effect on the expression of either *mini-white* or *LacZ*, confirming that the siRNA and piRNA pathways are not involved in the regulation of the Fab2L transgene. However, mutation of either *Dcr-1* or *Sb* resulted in a significant increase in expression of *mini-white* and *LacZ* ($p = 0.046$ and $p = 0.0046$ for *Dcr-1*, $p < 2 \times 10^{-5}$ and $p = 0.069$ for *Sb*, Tukey's HSD test after one-way ANOVA). We observed upregulation of both transgenic reporter genes, which are the products of two different transcripts whose expression is driven by the same promoter, thus indicating that the effects were at the level of transcription, rather than involving post-transcriptional regulation of *mini-white* by Dcr-1, or potential further downstream effects on eye morphogenesis by Sb. We therefore concluded that both Sb and Dcr-1 were likely to regulate transcription of the transgene indirectly.

Transcriptional regulation of the transgene is primarily controlled by PRC2, which deposits H3K27me3 to silence the transgene to varying degrees in the naïve, white and red epilines of Fab2L [29,33]. Recruitment of PRC2 to the transgene is achieved by *Pho*, which binds to a number of consensus sequence binding motifs present in the *Fab-7* regulatory element. Mutation of these binding motifs, the majority of which are present within a minimal Polycomb response element (PRE), has previously been shown to eliminate *Pho* binding and PRC2 recruitment, leading to a loss of epigenetic variation at the Fab2L locus and rendering TEI impossible [33]. Interference with PRC2 activity or recruitment would thus be one way of explaining the observed transcriptional changes caused by *Sb* and *Dcr-1* mutation.

To determine if *Dcr-1* and *Sb* mutation were affecting the activity of PRC2, we performed RT-qPCR to measure the PRC2 catalytic subunit *E(z)*, responsible for depositing H3K27me3 [58], and *Pho*, which recruits PRC2 to its targets [33,59]. *E(z)* expression was similar across all lines tested (figure 4*c*), whereas *Pho* was significantly downregulated in both the *Dcr-1* and *Sb* mutant lines ($p = 0.002$ and $p = 0.016$, respectively, Tukey's HSD after one-way ANOVA; figure 4*c*). This suggested a potential mechanism by which both *Dcr-1* and *Sb* mutations affect Fab2L eye colour, downregulating *Pho* and interfering with the binding of PRC2 to the *Fab-7* element within the transgene. Exactly how these effects on *Pho* expression are brought about is difficult to determine, but the involvement of miRNAs in many gene expression networks suggests the possibility that loss of Dcr-1 could lead to alterations in the regulation of *Pho*.

To our knowledge, this effect of Sb on *Pho* has not previously been reported. We hypothesized that this may be explained by the fact that the decrease in *Pho* expression is modest (around twofold) and therefore may not significantly affect the expression of most endogenous PRC2 targets, which are tightly regulated. To explore this, we measured the expression of two well-known PRC2 targets, *dachshund* (*dac*) and *Sex combs reduced* (*Scr*), in our mutant lines. Despite the decrease in *Pho* levels, we found no change in the expression of either *dac* or *Scr* in the *Sb* and *Dcr-1* mutant lines (electronic supplementary material, figure S7*a*,*b*). We also measured the expression of the transposable element *Blood*, which is silenced in a PRC2-independent manner. As expected, *Blood* levels remained unchanged in all mutant lines compared to wild-type, except for the *armi* mutant line where suppression of the piRNA pathway leads to massive upregulation of transposon expression ($p = 0.024$, Tukey's HSD test after one-way ANOVA; electronic supplementary material, figure S7c).

These results suggested that mutation of *Sb* and *Dcr-1* may not lead to widespread effects on PRC2 targets, despite their effect on *Pho* expression, and are therefore unlikely to manifest in other developmental phenotypes. We propose that this may be due to redundancy and reinforcement in endogenous gene expression networks providing a buffer to potential environmental or genetic perturbations [60]. Polycomb targets in particular are often coregulated in a manner that may be dependent on genomic location and three-dimensional (3D) chromatin organization [61]. As a transgene carrying a Polycomb-bound regulatory sequence divorced from its natural context, Fab2L may be more susceptible than endogenous loci to perturbation from mild disruptions that would normally be absorbed by these safeguards. Heterozygosity of *Pho*, for instance, is unlikely to have a significant effect on most Polycomb targets due not only to the presence of the remaining wild-type *Pho* copy but also redundancy with the related *Pho-like* and other PRC2 recruiters and coregulation with other targets [58,59,62]. Eye colour in Fab2L, on the other hand, reflects a stochastic pattern established by Pho-directed PRC2 binding in early development and maintained through adulthood. This fragile system is thus much more susceptible to disruption and may therefore be a more sensitive read-out of altered PRC2 recruitment. Moreover, the possibility of observing the effect across many individuals, each with a large number of ommatidia in their eyes, is more likely to reveal what in essence remains a mild effect on the average phenotype of the population (figure 3*d*,*e*).

Nevertheless, the ubiquity of *Sb[1]* as a marker may warrant caution in its use in certain cases. Indeed, the mild effects of a mutation may be exacerbated when combined with additional stressors such as extreme temperatures, something to which Polycomb targets may be particularly susceptible [63,64]. It may therefore be prudent to keep these effects in mind for future analyses involving Polycomb-regulated genes balanced on the TM3-Sb balancer, or otherwise linked to the *Sb[1]* mutation, and perhaps favour the use of the alternative TM3-Ser or other markers in these cases.

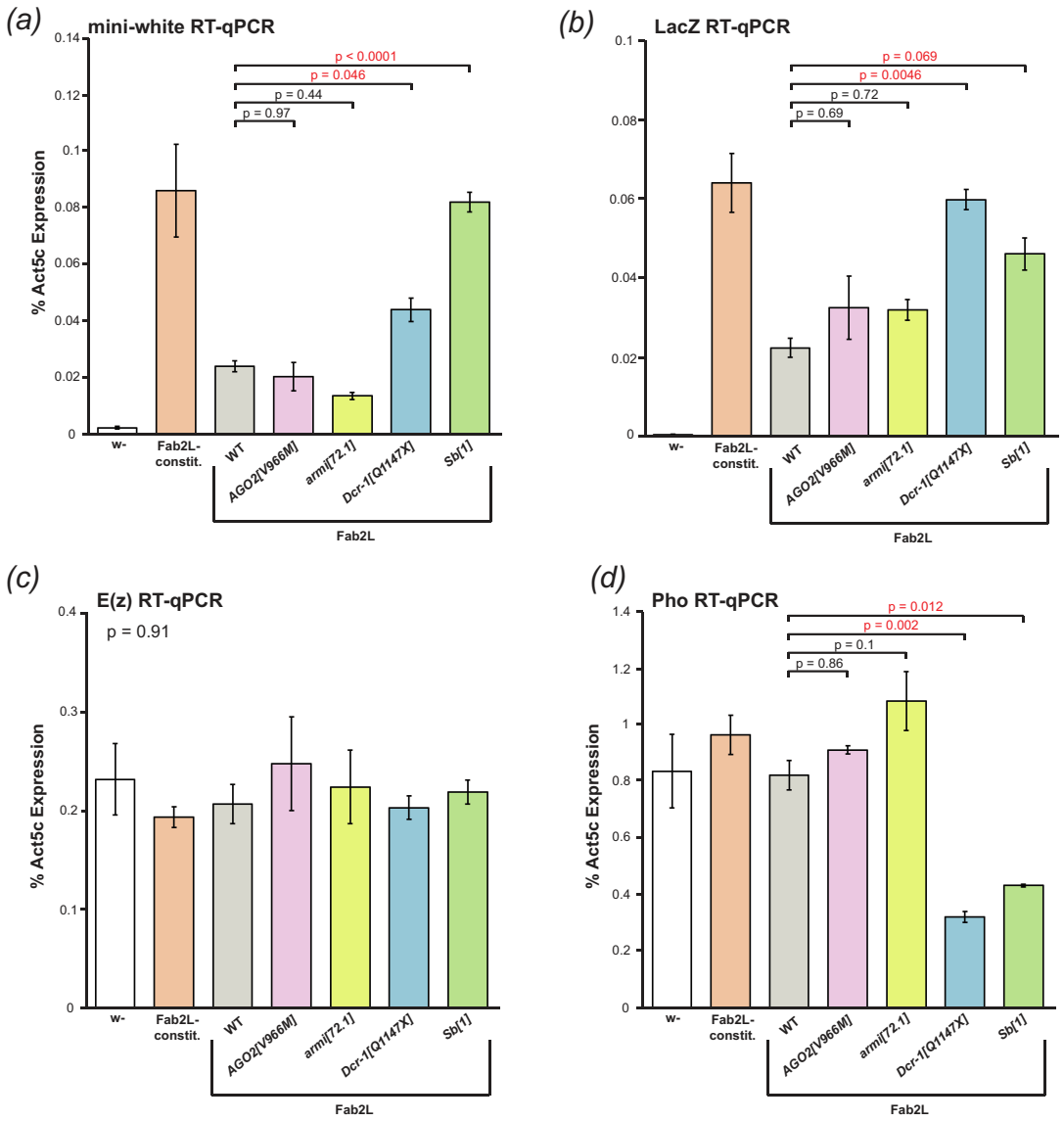

Figure 4. Mutation in *Dcr-1* and *Sb* increases transcription from the transgene and decreases expression of Pho. (*a–d*) RT-qPCR for expression of mini-white (*a*), LacZ (*b*), E(z) (*c*) and Pho (*d*) in embryos of the indicated genotypes. Expression was normalized to Act5C. Overall significance in the Fab2L samples was tested by one-way ANOVA, followed by pairwise comparison using Tukey's HSD in the event of significance (n.s. = $p > 0.1$).

2.6. Conclusion

In this study, we investigated the potential involvement of sRNAs in the transgenerational inheritance of a Polycomb-dependent epigenetic eye colour phenotype in *D. melanogaster*. Both sequencing and mutational analysis found no evidence for the involvement of either siRNAs or piRNAs in the establishment or maintenance of heritable epigenetic differences between individuals. These results provide further evidence that histone modifications, in this particular case H3K27me3, can be inherited transgenerationally in the absence of any other associated mark, encouraging further work to elucidate the exact mechanism by which this inheritance occurs. We identified indirect effects of the miRNA pathway on the expression of PRC2 component *Pho*, with interesting implications for understanding the control of PRC2-mediated regulation during development. Moreover, we also discovered an effect on *Pho* of the *Sb[1]* mutation, highlighting a previously unknown interaction between this marker gene and the Polycomb silencing pathway.

3. Material and methods

3.1. Fly stocks and culture

Flies were raised in standard cornmeal yeast extract media. Standard temperature was 21°C, with the exception of egg laying for RNA extraction, which was performed at 18°C. The Fab2L and Fab2L; *Fab7[1]* lines were described by Bantignies *et al*. [30]. The Fab2L, *black[1]* line and pre-established Fab2L epilines (Fab2L-R* and Fab2L-W*) were described by Ciabrelli *et al*. [29], while the Fab2L-constit. (also called Fab2L-INS-PRE) was described by Fitz-James *et al*. [33].

Fab2L, *black[1] ; Trl*^{R85}/TM6, Fab2L, *black[1]; E(z)*^{731}/TM3-sb and Fab2L, *black[1]; Sb[1]*/TM3-Ser flies were described by Ciabrelli *et al*. [29] and were crossed together to generate Fab2L, *black[1]; Trl*^{R85}/TM3-Ser, Fab2L, *black[1]; E(z)*^{731}/TM3-Ser, Fab2L, *black[1]; +*/TM3-Sb and Fab2L, *black[1]; +*/TM3-Ser.

Lines bearing the mutations *AGO2[V966M]* (BL32062), *armi[72.1]* (BL8544), *Dcr−1[Q1147X]* (BL32066), *mael [r20]* (BL8516) and *AGO3[t3]* (BL28270) were ordered from the Bloomington Drosophila Stock Center and crossed with Fab2L, *black[1]; Sb[1]*/TM3-Ser to generate the balanced lines.

To obtain homozygous mutant embryos, the above-mentioned mutant lines were balanced on the TM3, Sb, Kr-GFP (TKG) balancer chromosome, described by Casso *et al*. [65], by crossing them with *Pc*/TKG flies gifted by the Cavalli lab. The TKG balancer contains a fluorescent GFP marker expressed under control of the *krüppel* promoter, giving a distinct GFP pattern in mid to late embryos, thus allowing for the selection of homozygous embryos (see below).

3.2. Embryo collection

For both RNA extraction and FISH, flies were put in cages with yeasted apple juice agar plates for egg laying. Embryos were collected and washed in dH_2O before dechorionation with bleach. Embryos were collected either at stages 12–13 to allow time for sorting or stages 14–15 if proceeding directly to RNA extraction or FISH. Homozygous mutant embryos were obtained by sorting for GFP negative (or very strong GFP expression in the case of *Sb* mutants) embryos after dechorionation and kept in dH_2O or buffer A until ready. For RNA extraction, some embryos were stored at −20°C prior to extraction.

3.3. RNA extraction

A minimum of 20 embryos per sample were washed in DEPC-treated H_2O and pelleted with gentle centrifugation at 4000*g* for 2 min. Embryos were then homogenized in 50 µl Trizol reagent using a disposable pestle and then incubated at room temperature for 5 min in a total volume of 1 ml Trizol. Samples were mixed with 200 µl chloroform, incubated 2 min at room temperature and centrifuged 12 000*g* for 15 min at 4°C. The aqueous supernatant was taken and RNA precipitated with 500 µl isopropanol for 10 min at 4°C. Samples were centrifuged at 12 000*g* for 10 min, washed in 1 ml 75% EtOH and centrifuged again. The pellet was air-dried and resuspended in 25 µl RNase-free H_2O. Residual DNA was removed using the DNA-free DNA Removal kit (Ambion), and RNA concentration was determined using a Qubit spectrophotometer.

3.4. Small RNA sequencing

sRNA library preparation and sequencing were performed by Novogene using an Illumina Novaseq 6000 using 50 bp single-end reads. Starting from raw fastq files, adapters were trimmed using fastx_toolkit, and sequences were aligned to the *Drosophila* genome (dm6) and a custom genome built from the Fab2L fasta sequence using Bowtie-build, using 0 mismatches and reporting one alignment per read. Alignment files in sam format were converted to bam files using samtools, and bam files were converted to bed files using bamToBed. The resulting bed files were then used as input for R scripts to collate the length and first nucleotide to produce plots. Hairpin-mapping sRNAs were analysed by selecting reads that overlapped with annotated hairpin sRNA loci (hpRNA) extracted from the gff3 file for the *Drosophila* genome downloaded from FlyBase. piRNA cluster-mapping sRNAs were extracted by selecting all reads that overlapped with the *Drosophila* piRNA cluster positions downloaded from https://www.smallrnagroup.uni-mainz.de/piRNAclusterDB/). R Code to reproduce the plots is available via the Sarkies Lab GitHub page (SarkiesLab/Fab2LsRNA).

3.5. Quantitative reverse transcription polymerase chain reaction

In total, 200 ng RNA was converted to cDNA using the high-capacity RNA-to-cDNA kit (Applied Biosystems) before dilution 1:40. Samples were then subjected to qPCR in triplicate on a CFX 384 Real-time PCR System (Bio-Rad) with a total volume of 10 µl per well (5 µl cDNA and 5 µl iTaq universal SYBR green supermix containing 1 µM of each primer). *Cq* values were averaged across the three triplicates and normalized to Act5C.

3.6. Fluorescence *in situ* hybridization

Two-colour 3D FISH was performed as previously described [66] (for a detailed protocol, see [67]). Embryos collected as indicated above were fixed at stages 14–15 in buffer A (60 mM KCl; 15 mM NaCl; 0.5 mM spermidine; 0.15 mM spermine; 2 mM EDTA; 0.5 mM EGTA; 15 mM PIPES, pH 7.4) with 4% paraformaldehyde for 25 min in the presence of heptane then devitellinized by adding methanol to the heptane phase, extracted and washed three times in methanol. Embryos were kept for a maximum of 4 months in methanol at 4°C before proceeding to FISH. Fixed embryos were sequentially re-hydrated in phosphate-buffered Tween (PBT), consisting of phosphate-buffered (PBS) with 0.1% Tween 20, before being treated with 100–200 µg ml^{-1} RNaseA in PBT for 2 h at room temperature. Embryos were then sequentially transferred into a pre-hybridization mixture (pHM: 50% formamide; 4XSSC; 100 mM NaH_2PO_4, pH 7.0; 0.1% Tween 20). Embryonic DNA was denatured in pHM at 80°C for 15 min. The pHM was removed, and denatured probes diluted in the FISH hybridization buffer (FHB: 10% dextran sulfate; 50% deionized formamide; 2XSSC; 0.5 mg ml^{-1} Salmon Sperm DNA) were added to the tissues without prior cooling. Hybridization was performed at 37°C overnight with gentle agitation. Post-hybridization washes

were performed, starting with 50% formamide, 2XSSC, 0.3% 3-[(3-cholamidopropyl)dimethylammonio]-1-propanesulfonate (CHAPS) and sequentially returning to PBT. After an additional wash in PBS-Tr, DNA was counterstained with DAPI (at a final concentration of 0.1 ng μl^{-1}) in PBT, and embryos were mounted with ProLong Gold Antifade (Invitrogen).

FISH probes for the 37B and 89E regions were made from a previous design described by Ciabrelli *et al*. [29]. For each region, six non-overlapping probes of between 1.2 and 1.7 kb covering an area of approximately 12 kb were generated using the FISH Tag DNA kit with Alexa Fluor 555 or Alexa Fluor 647 dyes (Invitrogen Life Technologies). In total, 100 ng of each probe was added to the 30 µl of FHB for hybridization.

3.7. Microscopy and image analysis

For the FISH, the 3D distances between 37B and 89E loci were acquired and measured as follows: due to somatic pairing of homologous chromosomes in *Drosophila*, the majority of the nuclei in embryos show a single FISH spot for each probe. In the cases of non-overlap FISH signals between homologues, the closest distance between the centres of the two probes was considered. To measure distances, 3D stacks were collected from three different embryos. Optical sections were collected at 0.3–0.5 µm intervals along the *Z*-axis using a Zeiss LSM980 microscope at the Micron Imaging facility. Relative 3D distances between FISH signals were measured in approximately 100 nuclei per 3D stack using Imaris software (Oxford Instruments) and plotted in R using the ggplot2 package.

3.8. Statistical analysis

Statistical analysis was performed in R using the Tidyverse package. Fab2L–*Fab7* distance measurements from the same embryo were assigned an embryo ID, and distributions were tested by two-way ANOVA with the genotype and embryo ID as parameters, before pairwise comparison using Tukey's HSD. RT-qPCR data were tested by one-way ANOVA and, in the case of significance, compared pairwise with Tukey's HSD. Fisher's exact test was used to compare the distribution of eye colour between the F2 of paramutation crosses. *P* values were adjusted by Bonferroni correction. Given the correction applied to all *p* values, 0.1 was taken as the upper bound for significance, with all values below being reported.

Ethics. This work did not require ethical approval from a human subject or animal welfare committee.

Data accessibility. Small RNA sequencing has been submitted to the SRA; the accession is PRJNA1210574.

Supplementary material is available online [68].

Declaration of AI use. We have not used AI-assisted technologies in creating this article.

Authors' contributions. M.F.-J.: conceptualization, formal analysis, resources; P.Sp.: investigation, methodology, resources, software, writing—original draft, writing—review and editing; C.P.: investigation, methodology, project administration, visualization, writing—original draft, writing—review and editing; P.Sa.: conceptualization, formal analysis, funding acquisition, validation, visualization, writing—original draft, writing—review and editing.

All authors gave final approval for publication and agreed to be held accountable for the work performed therein.

Conflict of interests. We declare we have no competing interests.

Funding. The research presented in this study was funded by the John Fell Fund (Grant No 0011417) and the Department of Biochemistry (University of Oxford). C.P. was funded by an Undergraduate vacation studentship from the Biochemical Society.

Acknowledgements. We thank the Cavalli lab (Institute of Human Genetics, University of Montpellier and CNRS) for the gift of the *Drosophila* lines used in this study. We also thank the Micron Imaging Facility and the Jansen lab (Department of Biochemistry, University of Oxford) for the use of equipment.

References

1. Allis CD, Jenuwein T. 2016 The molecular hallmarks of epigenetic control. *Nat. Rev. Genet*. **17**, 487–500. (doi:10.1038/nrg.2016.59)
2. Bogdanović O, Veenstra GJC. 2009 DNA methylation and methyl-CpG binding proteins: developmental requirements and function. *Chromosoma* **118**, 549–565. (doi:10.1007/s00412-009-0221-9)
3. Bannister AJ, Kouzarides T. 2011 Regulation of chromatin by histone modifications. *Cell Res*. **21**, 381–395. (doi:10.1038/cr.2011.22)
4. Gou LT, Zhu Q, Liu MF. 2023 Small RNAs: an expanding world with therapeutic promises. *Fundam. Res*. **3**, 676–682. (doi:10.1016/j.fmre.2023.03.003)
5. Bonasio R, Tu S, Reinberg D. 2010 Molecular signals of epigenetic states. *Science* **330**, 612–616. (doi:10.1126/science.1191078)
6. Bošković A, Rando OJ. 2018 Transgenerational epigenetic inheritance. *Annu. Rev. Genet*. **52**, 21–41. (doi:10.1146/annurev-genet-120417-031404)
7. Fitz-James MH, Cavalli G. 2022 Molecular mechanisms of transgenerational epigenetic inheritance. *Nat. Rev. Genet*. **23**, 325–341. (doi:10.1038/s41576-021-00438-5)
8. Rechavi O, Houri-Ze'evi L, Anava S, Goh WSS, Kerk SY, Hannon GJ, Hobert O. 2014 Starvation-induced transgenerational inheritance of small RNAs in *C. elegans*. *Cell* **158**, 277–287. (doi:10.1016/j.cell.2014.06.020)
9. Schott D, Yanai I, Hunter CP. 2014 Natural RNA interference directs a heritable response to the environment. *Sci. Rep*. **4**, 7387. (doi:10.1038/srep07387)
10. Kaletsky R, Moore RS, Vrla GD, Parsons LR, Gitai Z, Murphy CT. 2020 *C. elegans* interprets bacterial non-coding RNAs to learn pathogenic avoidance. *Nature* **586**, 445–451. (doi:10.1038/s41586-020-2699-5)
11. Posner R *et al*. 2019 Neuronal small RNAs control behavior transgenerationally. *Cell* **177**, 1814–1826.(doi:10.1016/j.cell.2019.04.029)
12. Brennecke J, Malone CD, Aravin AA, Sachidanandam R, Stark A, Hannon GJ. 2008 An epigenetic role for maternally inherited piRNAs in transposon silencing. *Science* **322**, 1387–1392. (doi:10.1126/science.1165171)

13. Schwartz-Orbach L, Zhang C, Sidoli S, Amin R, Kaur D, Zhebrun A, Ni J, Gu SG. 2020 *Caenorhabditis elegans* nuclear RNAi factor SET-32 deposits the transgenerational histone modification, H3K23me3. *eLife* **9**, e54309. (doi:10.7554/elife.54309)
14. Lev I, Rechavi O. 2020 Germ granules allow transmission of small RNA-based parental responses in the 'germ plasm'. *iScience* **23**, 101831. (doi:10.1016/j.isci.2020.101831)
15. Lev I *et al*. 2019 Germ granules govern small RNA inheritance. *Curr. Biol*. **29**, 2880–2891.(doi:10.1016/j.cub.2019.07.054)
16. Czech B, Munafò M, Ciabrelli F, Eastwood EL, Fabry MH, Kneuss E, Hannon GJ. 2018 piRNA-guided genome defense: from biogenesis to silencing. *Annu. Rev. Genet*. **52**, 131–157. (doi:10.1146/annurev-genet-120417-031441)
17. Carthew RW, Sontheimer EJ. 2009 Origins and mechanisms of miRNAs and siRNAs. *Cell* **136**, 642–655. (doi:10.1016/j.cell.2009.01.035)
18. Carthew RW, Agbu P, Giri R. 2017 MicroRNA function in *Drosophila melanogaster*. *Semin. Cell Dev. Biol*. **65**, 29–37. (doi:10.1016/j.semcdb.2016.03.015)
19. Onishi R, Yamanaka S, Siomi MC. 2021 piRNA- and siRNA-mediated transcriptional repression in *Drosophila*, mice, and yeast: new insights and biodiversity. *EMBO Rep*. **22**, e53062. (doi:10.15252/embr.202153062)
20. Huang X, Fejes Tóth K, Aravin AA. 2017 piRNA biogenesis in *Drosophila melanogaster*. *Trends Genet*. **33**, 882–894. (doi:10.1016/j.tig.2017.09.002)
21. Parhad SS, Theurkauf WE. 2019 Rapid evolution and conserved function of the piRNA pathway. *Open Biol*. **9**, 180181. (doi:10.1098/rsob.180181)
22. Luteijn MJ, van Bergeijk P, Kaaij LJT, Almeida MV, Roovers EF, Berezikov E, Ketting RF. 2012 Extremely stable Piwi-induced gene silencing in *Caenorhabditis elegans*. *EMBO J*. **31**, 3422–3430. (doi:10.1038/emboj.2012.213)
23. Ashe A *et al*. 2012 piRNAs can trigger a multigenerational epigenetic memory in the germline of *C. elegans*. *Cell* **150**, 88–99. (doi:10.1016/j.cell.2012.06.018)
24. Shirayama M, Seth M, Lee HC, Gu W, Ishidate T, Conte D, MelloCC. 2012 piRNAs initiate an epigenetic memory of nonself RNA in the *C. elegans* germline. *Cell* **150**, 65–77. (doi:10.1016/j.cell.2012.06.015)
25. De Vanssay A, Bougé AL, Boivin A, Hermant C, Teysset L, Delmarre V, Antoniewski C, Ronsseray S. 2012 Paramutation in *Drosophila* linked to emergence of a piRNA-producing locus. *Nature* **490**, 112–115. (doi:10.1038/nature11416)
26. Scarpa A, Kofler R. 2023 The impact of paramutations on the invasion dynamics of transposable elements. *Genetics* **225**, iyad181. (doi:10.1093/genetics/iyad181)
27. Sun L, Mu Y, Xu L, Han X, Gu W, Zhang M. 2023 Transgenerational inheritance of wing development defects in *Drosophila melanogaster* induced by cadmium. *Ecotoxicol. Environ. Saf*. **250**, 114486. (doi:10.1016/j.ecoenv.2022.114486)
28. Seong KH, Li D, Shimizu H, Nakamura R, Ishii S. 2011 Inheritance of stress-induced, ATF-2-dependent epigenetic change. *Cell* **145**, 1049–1061. (doi:10.1016/j.cell.2011.05.029)
29. Ciabrelli F *et al*. 2017 Stable Polycomb-dependent transgenerational inheritance of chromatin states in *Drosophila*. *Nat. Genet*. **49**, 876–886. (doi:10.1038/ng.3848)
30. Bantignies F, Grimaud C, Lavrov S, Gabut M, Cavalli G. 2003 Inheritance of polycomb-dependent chromosomal interactions in *Drosophila*. *Genes Dev*. **17**, 2406–2420. (doi:10.1101/gad.269503)
31. Zink D, Paro R. 1995 *Drosophila* polycomb-group regulated chromatin inhibits the accessibility of a trans-activator to its target DNA. *EMBO J*. **14**, 5660–5671. (doi:10.1002/j.1460-2075.1995.tb00253.x)
32. Allshire RC, Ekwall K. 2015 Epigenetic regulation of chromatin states in *Schizosaccharomyces pombe*. *Cold Spring Harb. Perspect. Biol*. **7**, 1–25. a018770. (doi:10.1101/cshperspect.a018770)
33. Fitz-James MH, Sabarís G, Sarkies P, Bantignies F, Cavalli G. 2024 Interchromosomal contacts between regulatory regions trigger stable transgenerational epigenetic inheritance in *Drosophila*. *Mol. Cell* (doi:10.1016/j.molcel.2024.11.021)
34. Ronsseray S. 2015 Paramutation phenomena in non-vertebrate animals. *Semin. Cell Dev. Biol*. **44**, 39–46. (doi:10.1016/j.semcdb.2015.08.009)
35. Cecere G. 2021 Small RNAs in epigenetic inheritance: from mechanisms to trait transmission. *FEBS Lett*. **595**, 2953–2977. (doi:10.1002/1873-3468.14210)
36. Grimaud C, Bantignies F, Pal-Bhadra M, Ghana P, Bhadra U, Cavalli G. 2006 RNAi components are required for nuclear clustering of polycomb group response elements. *Cell* **124**, 957–971. (doi:10.1016/j.cell.2006.01.036)
37. Kim K, Lee YS, Carthew RW. 2007 Conversion of pre-RISC to holo-RISC by Ago2 during assembly of RNAi complexes. *RNA* **13**, 22–29. (doi:10.1261/rna.283207)
38. Cook HA, Koppetsch BS, Wu J, Theurkauf WE. 2004 The *Drosophila* SDE3 homolog armitage is required for oskar mRNA silencing and embryonic axis specification. *Cell* **116**, 817–829. (doi:10.1016/s0092-8674(04)00250-8)
39. Vagin VV, Sigova A, Li C, Seitz H, Gvozdev V, Zamore PD. 2006 A distinct small RNA pathway silences selfish genetic elements in the germline. *Science* **313**, 320–324. (doi:10.1126/science.1129333)
40. Olivieri D, Sykora MM, Sachidanandam R, Mechtler K, Brennecke J. 2010 An *in vivo* RNAi assay identifies major genetic and cellular requirements for primary piRNA biogenesis in *Drosophila*. *EMBO J*. **29**, 3301–3317. (doi:10.1038/emboj.2010.212)
41. Lee YS, Nakahara K, Pham JW, Kim K, He Z, Sontheimer EJ, Carthew RW. 2004 Distinct roles for *Drosophila* dicer-1 and dicer-2 in the siRNA/miRNA silencing pathways. *Cell* **117**, 69–81. (doi:10.1016/s0092-8674(04)00261-2)
42. Hollick JB. 2017 Paramutation and related phenomena in diverse species. *Nat. Rev. Genet*. **18**, 2016. (doi:10.1038/nrg.2016.115)
43. Pilu R. 2015 Paramutation phenomena in plants. *Semin. Cell Dev. Biol*. **44**, 2–10. (doi:10.1016/j.semcdb.2015.08.015)
44. Müller J *et al*. 2002 Histone methyltransferase activity of a *Drosophila* Polycomb group repressor complex. *Cell* **111**, 197–208. (doi:10.1016/s0092-8674(02)00976-5)
45. Farkas G, Gausz J, Galloni M, Reuter G, Gyurkovics H, Karch F. 1994 The Trithorax-like gene encodes the *Drosophila* GAGA factor. *Nature* **371**, 806–808. (doi:10.1038/371806a0)
46. Hermant C, Boivin A, Teysset L, Delmarre V, Asif-Laidin A, van den Beek M, Antoniewski C, Ronsseray S. 2015 Paramutation in *Drosophila* requires both nuclear and cytoplasmic actors of the piRNA pathway and induces cis-spreading of piRNA production. *Genetics* **201**, 1381–1396. (doi:10.1534/genetics.115.180307)
47. Clegg NJ, Frost DM, Larkin MK, Subrahmanyan L, Bryant Z, Ruohola-Baker H. 1997 *Maelstrom* is required for an early step in the establishment of *Drosophila* oocyte polarity: posterior localization of *grk* mRNA. *Development* **124**, 4661–4671. (doi:10.1242/dev.124.22.4661)
48. Li X, Cassidy JJ, Reinke CA, Fischboeck S, Carthew RW. 2009 A microRNA imparts robustness against environmental fluctuation during development. *Cell* **137**, 273–282. (doi:10.1016/j.cell.2009.01.058)
49. Miller DE, Cook KR, Arvanitakis AV, Hawley RS. 2016 Third chromosome balancer inversions disrupt protein-coding genes and influence distal recombination events in *Drosophila melanogaster*. *G3 Genes, Genomes, Genet* **6**, 1959–1967. (doi:10.1534/g3.116.029330)
50. Thomas U, Jönsson F, Speicher SA, Knust E. 1995 Phenotypic and molecular characterization of SerD, a dominant allele of the *Drosophila* gene Serrate. *Genetics* **139**, 203–213. (doi:10.1093/genetics/139.1.203)
51. Hammonds AS, Fristrom JW. 2006 Mutational analysis of *Stubble-stubbloid* gene structure and function in *Drosophila* leg and bristle morphogenesis. *Genetics* **172**, 1577–1593. (doi:10.1534/genetics.105.047100)
52. Bayer CA, Halsell SR, Fristrom JW, Kiehart DP, von Kalm L. 2003 Genetic interactions between the RhoA and stubble-stubbloid loci suggest a role for a type II transmembrane serine protease in intracellular signaling during *Drosophila* imaginal disc morphogenesis. *Genetics* **165**, 1417–1432. (doi:10.1093/genetics/165.3.1417)

53. Ward RE, Evans J, Thummel CS. 2003 Genetic modifier screens in *Drosophila* demonstrate a role for Rho1 signaling in ecdysone-triggered imaginal disc morphogenesis. *Genetics* **165**, 1397–1415. (doi:10.1093/genetics/165.3.1397)
54. Chen GC, Gajowniczek P, Settleman J. 2004 Rho-LIM kinase signaling regulates ecdysone-induced gene expression and morphogenesis during *Drosophila* metamorphosis. *Curr. Biol.* **14**, 309–313. (doi:10.1016/j.cub.2004.01.056)
55. Ibrahim DM, Biehs B, Kornberg TB, Klebes A. 2013 Microarray comparison of anterior and posterior *Drosophila* wing imaginal disc cells identifies novel wing genes. *G3 Genes,Genomes, Genet* **3**, 1353–1362. (doi:10.1534/g3.113.006569)
56. Condic ML, Fristrom D, Fristrom JW. 1991 Apical cell shape changes during *Drosophila* imaginal leg disc elongation: a novel morphogenetic mechanism. *Development* **111**, 23–33. (doi:10.1242/dev.111.1.23)
57. Uyehara CM, McKay DJ. 2019 Direct and widespread role for the nuclear receptor EcR in mediating the response to ecdysone in *Drosophila*. *Proc. Natl Acad. Sci. USA* **116**, 9893–9902. (doi:10.1073/pnas.1900343116)
58. Schuettengruber B, Bourbon HM, Di Croce L, Cavalli G. 2017 Genome regulation by polycomb and trithorax: 70 years and counting. *Cell* **171**, 34–57. (doi:10.1016/j.cell.2017.08.002)
59. Brown JL, Fritsch C, Mueller J, Kassis JA. 2003 The *Drosophila pho-like* gene encodes a YY1-related DNA binding protein that is redundant with pleiohomeotic in homeotic gene silencing. *Development* **130**, 285–294. (doi:10.1242/dev.00204)
60. MacNeil LT, Walhout AJM. 2011 Gene regulatory networks and the role of robustness and stochasticity in the control of gene expression. *Genome Res*. **21**, 645–657. (doi:10.1101/gr.097378.109)
61. Entrevan M, Schuettengruber B, Cavalli G. 2016 Regulation of genome architecture and function by polycomb proteins. *Trends Cell Biol*. **26**, 511–525. (doi:10.1016/j.tcb.2016.04.009)
62. Schuettengruber B *et al*. 2014 Cooperativity, specificity, and evolutionary stability of polycomb targeting in *Drosophila*. *Cell Rep*. **9**, 219–233. (doi:10.1016/j.celrep.2014.08.072)
63. Voigt S, Kost L. 2021 Differences in temperature-sensitive expression of PcG-regulated genes among natural populations of *Drosophila melanogaster*. *G3 Genes,Genomes, Genet* **11**, jkab237. (doi:10.1093/g3journal/jkab237)
64. Ogiyama Y, Schuettengruber B, Papadopoulos GL, Chang JM, Cavalli G. 2018 Polycomb-dependent chromatin looping contributes to gene silencing during *Drosophila* development. *Mol. Cell* **71**, 73–88.(doi:10.1016/j.molcel.2018.05.032)
65. Casso D, Ramı´rez-Weber FA, Kornberg TB. 1999 GFP-tagged balancer chromosomes for *Drosophila melanogaster*. *Mech. Dev*. **88**, 229–232. (doi:10.1016/s0925-4773(99)00174-4)
66. Bantignies F, Roure V, Comet I, Leblanc B, Schuettengruber B, Bonnet J, Tixier V, Mas A, Cavalli G. 2011 Polycomb-dependent regulatory contacts between distant hox loci in *Drosophila*. *Cell* **144**, 214–226. (doi:10.1016/j.cell.2010.12.026)
67. Bantignies F, Cavalli G. 2014 Topological organization of *Drosophila* hox genes using DNA fluorescent in situ hybridization. *Methods Mol. Biol.* **1196**, 103–120. (doi:10.1007/978-1-4939-1242-1_7)
68. Fitz-James M, Sparrow P, Paton C, Sarkies P. 2025 Supplementary material from: Polycomb-mediated transgenerational epigenetic inheritance of *Drosophila* eye colour is independent of small RNAs. Figshare (doi:10.6084/m9.figshare.c.7702725)